VI CONGRESSO NACIONAL DE ENGENHARIA MECÂNICA
VI NATIONAL CONGRESS OF MECHANICAL ENGINEERING
18 a 21 de agosto de 2010 – Campina Grande – Paraíba - Brasil
August 18 – 21, 2010 – Campina Grande – Paraíba – Brazil

USE OF A GENETIC ALGORITHM MODEL IN THE AERODYNAMIC OPTIMIZATION OF WIND TURBINE BLADES

Felipe José Vinaud, felipevinaud@gmail.com[1]
João Carlos Menezes, menezes@ita.br[2]
[1,2] ITA - Instituto Técnológico de Aeronáutica, Divisão de Engenharia Mecânica-Aeronáutica, CTA-ITA-IEM, Pça Mal. Eduardo Gomes n^o 50, 12228-900, São José dos Campos, SP, Brazil,

Abstract. *The demand for electric energy has increased dramatically in the last years while the environmental effects and the use of clean energies are a reality that must be taken into account in the buildup of the energetic matrix of a country. As a consequence, the need for reliable and efficient means for generating electricity has brought up the necessity of developing optimization methods in the design of many machines, including wind turbines. This paper presents the preliminary results of the work leading to a future genetic algorithm optimization of the cross section of wind turbine blades aiming at the maximum power coefficient (CP). Thus the objective of the the optimization is the minimization of the drag/lift ratio of a blade section. The PARSEC methodology was used to obtain a feasible geometry for the solution of the aerodynamic problem with only a few parameters. The panel method with a correction for viscosity effects is used for the solution of the flow field around the blade section. The results will allow for the choice of an approximate optimum geometry for the solution of a more complex CFD model in the future.*

Keywords: *Wind energy, Optimization, Genetic Algorithms, Aerodynamics*

1. INTRODUCTION

During recent years it has been observed an increase in the demand for electrical power. Thus, a more efficient generation of power is to be assessed in order to optimize the operation of horizontal axis wind turbines (HAWT) and increase the extraction of energy from the wind. With this aim, this work was proposed as a preliminary study of the running conditions of rotor blade geometry from an aerodynamic standpoint. For such, this article presents a simple study of the blade element theory used for determining the blade geometry taking into account phenomenon such as wake rotation. For attaining the drag to lift ratio, a simple vortex panel method is used to determine the lift coefficient. Thwaitet's and Headt's methods are used in order to determine skin friction coefficients for the airfoils. The total drag coefficient is calculated based in skin friction drag and form drag. The optimization procedure that will be implemented uses a parameterization scheme called PARSEC for obtaining 2D airfoil geometries based on useful geometric features such as leading edge radius and trailing edge cusp angle. This scheme makes it possible for the genetic algorithm code to choose geometry parameters that are more likely to give the maximum power coefficient (CP) for the respective blade element

2. AERODYNAMICS OF WIND TURBINES

2.1 Momentum Theory

A wind turbine rotor consists of airfoils that generate lift through the pressure difference across the airfoil. In momentum theory, the flow field around a wind turbine rotor, represented by an actuator disc, is determined using the conservation of linear and angular momentum. This flow field is characterized by axial and angular induction factors that are a function of the rotor power extraction and thrust. According to Manwell *et al.* (2002), the geometry of the rotor and the lift and drag characteristics of the rotor airfoils can then be used to determine either the rotor shape, if certain performance parameters are known, or rotor performance, if the blade shape has already been defined. The axial and angular induction factors are defined as:

$$a = \frac{U_1 - U_2}{U_1} \tag{1}$$

$$a' = \frac{\omega}{2\Omega} \tag{2}$$

where U_1 is the free stream velocity, $U2$ is the velocity at the rotor disc, ω is the angular velocity imparted to the flow stream and Ω is the velocity of the wind turbine rotor (see Fig. 1).

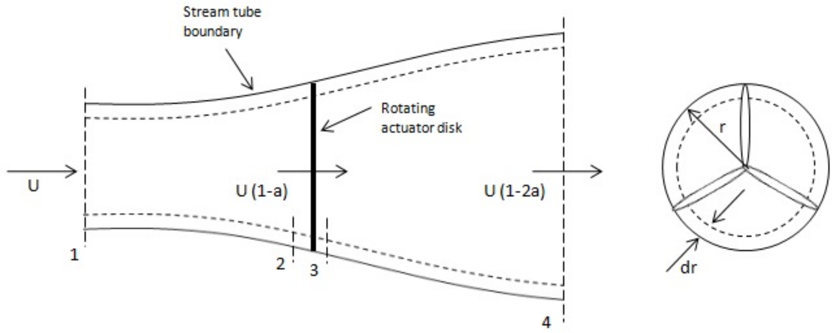

Figure 1. Geometry of rotor analysis; U, velocity of undisturbed air; a, induction factor; r, radius.

The forces on a wind turbine blade can be derived considering the conservation of momentum. Considering the annular control volume shown in Fig. 1, the axial and angular induction factors are assumed to be functions of the radius r. From the conservation of linear momentum of the control volume of radius r and thickness dr the equation of the differential contribution to the thrust is:

$$dT = \rho U^2 4a\,(1-a)\,\pi r dr \tag{3}$$

Similarly from the conservation of angular momentum, the differential torque Q, imparted to the blades (equally and oppositely to the air) is:

$$dQ = 4a'\,(1-a)\,\rho U \pi r^3 \Omega dr \tag{4}$$

2.2 Blade Element Theory

The forces on the blades of a wind turbine can also be expressed as a function of lift and drag coefficients and the angle of attack. As shown in Fig. 2, the blade is assumed to be divided into N elements. Furthermore, it is assumed that there is no aerodynamic interaction between the elements and that the forces on the blades are determined solely by the lift and drag characteristics of the airfoil shape of the blades.

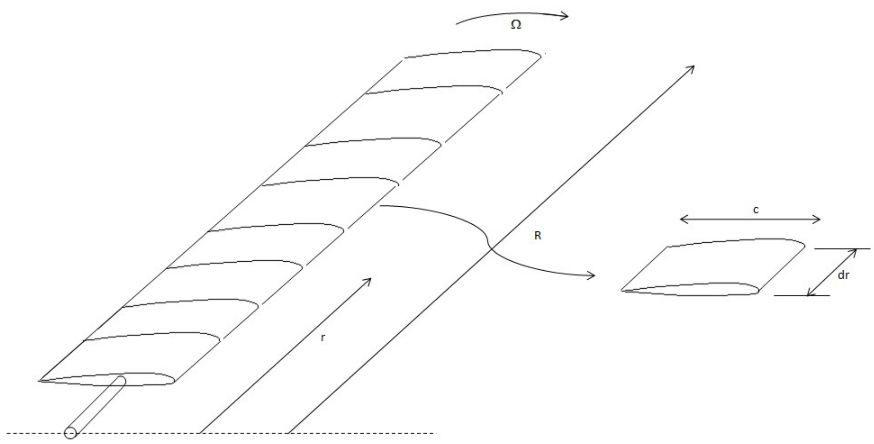

Figure 2. Schematic of blade elements: c, airfoil chord length; dr, radial length of element; R, rotor radius; Ω, angular velocity of rotor.

The lift and drag forces of a blade section are perpendicular and parallel, respectively, to an effective, or relative wind. The relative wind is the sum of the wind velocity at the rotor, $U(1-a)$, and the wind velocity due to rotation of the blade. This rotational component is the vector sum of the blade section velocity, Ωr, and the induced angular velocity at the blades from conservation of angular momentum, $\omega r/2$, or

$$\Omega r + (\omega/2)\,r = \Omega r + \Omega a' r = \Omega r\,(1+a') \tag{5}$$

The the relationships of the various forces, angles and velocities at the blade, looking down from the blade tip, is shown in Fig. 3. Here, dF_L is the incremental lift force, dF_D is the incremental drag force, dF_N is the incremental force normal to the plane of rotation (contributing to thrust), and dF_T is the incremental force tangential to the circle swept by the rotor (force creating useful torque).

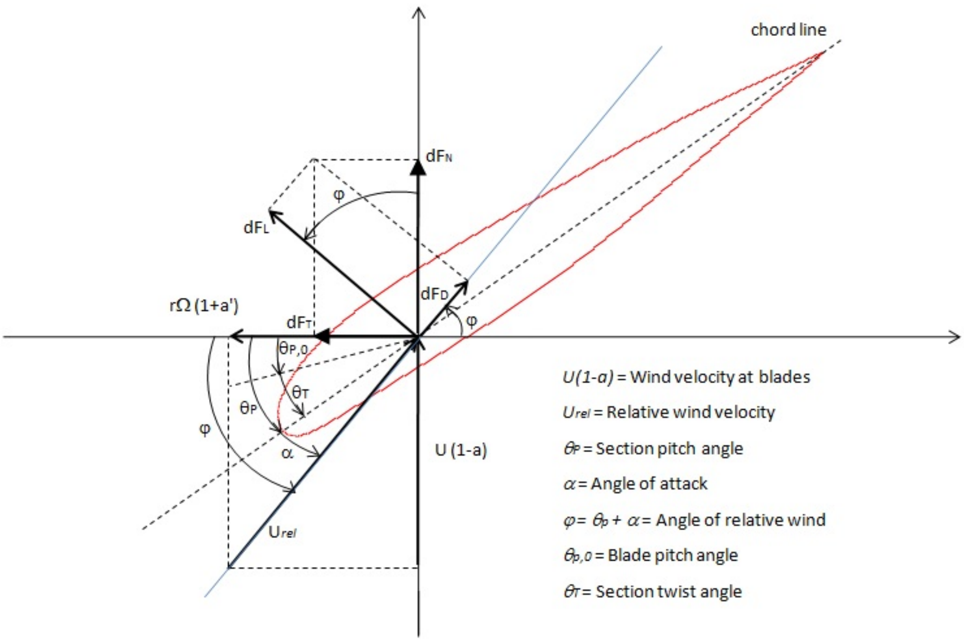

Figure 3. Blade geometry for analysis of a HAWT.

The blade twist angle, θ_T, is defined relative to the blade tip. Therefore

$$\theta_T = \theta_P - \theta_{P0} \tag{6}$$

The twist angle is a function of the blade geometry, whereas θ_P changes if the position of the blade, $\theta_{p,0}$, is changed. Also, the angle of relative wind is the sum of the section pitch angle and the angle of attack:

$$\varphi = \theta_P + \alpha \tag{7}$$

From Fig. 3, one can determine the following relationships:

$$\tan\varphi = \frac{U\left(1-a\right)}{\Omega r\left(1+a'\right)} = \frac{1-a}{\left(1+a'\right)\lambda_r} \tag{8}$$

where λ_r is the local speed ratio or the ratio of rotor speed at some intermediate radius to the wind speed $\lambda_r = \Omega r/U$. Also:

$$\begin{aligned}
U_{rel} &= U\left(1-a\right)/\sin\varphi && (9)\\
dF_L &= C_l\frac{1}{2}\rho U_{rel}^2 cdr && (10)\\
dF_d &= C_d\frac{1}{2}\rho U_{rel}^2 cdr && (11)\\
dF_N &= dF_L\cos\varphi + dF_D\sin\varphi && (12)\\
dF_T &= dF_L\sin\varphi - dF_D\cos\varphi && (13)
\end{aligned}$$

If the rotor has B blades, the total normal force on the section at a distance r from the center is given by

$$dF_N = B\frac{1}{2}\rho U_{rel}^2\left(C_l\cos\varphi + C_d\sin\varphi\right)cdr \tag{14}$$

The differential torque due to the tangential force operating at a distance r from the center is given by

$$dQ = B\cdot r\cdot dF_T \tag{15}$$

so

$$dQ = B\frac{1}{2}\rho U_{rel}^2 \left(C_l \sin\varphi - C_d \cos\varphi\right) crdr \tag{16}$$

Note that the effect of drag is to decrease torque and hence power, but to increase thrust loading.

2.3 Generalized Rotor Design Procedure

The procedure for determining the rotor design for specific conditions begins with the choice of various rotor parameters and the choice of an airfoil. The final blade shape and performance are determined iteratively. The steps in determining the blade design follow:

Determine basic rotor parameters

1. Begin deciding the power, P, and the wind speed, U. Include the effect of a probable C_p and efficiencies η of various components. The radius R of the rotor may be estimated from:

$$P = C_p \eta 1/2 \rho \pi R^2 U^3 \tag{17}$$

2. For electric power generation choose a tip speed ratio between 4 and 10. The higher speed machines use less material in the blades and have smaller gearboxes, but require more sophisticated airfoils. Usually for $\lambda > 4$ the number of blades B must be 3.

3. Select an airfoil. If $\lambda > 3$ a more aerodynamic shape must be used.

Define the blade shape

4. From the airfoil curves $C_{l,design}$ vs. $\alpha_{l,design}$ and $C_{d,design}$ vs. $\alpha_{l,design}$ chose the design aerodynamic conditions such that $C_{d,design}/C_{l,design}$ is at a minimum for each blade section

5. Divide the blade into N elements (usually 10-20). Use the following relations to estimate the shape of the *i*th blade with a midpoint of radius r_i:
local tip speed ratio

$$\lambda_{r,i} = \lambda(r_i/R) \tag{18}$$

local angle of relative wind

$$\varphi_i = tan^{-1}\left(\frac{2}{3\lambda_{r,i}}\right) \tag{19}$$

element chord length

$$c_i = \frac{8\pi r_i}{BC_{l,i}}\left(1 - \cos\varphi_i\right) \tag{20}$$

element twist angle

$$\theta_{T,i} = \theta p, i - \theta p, 0 \tag{21}$$

also:

$$\varphi_i = \theta_{p,i} + \alpha_{design,i} \tag{22}$$

6. Using the optimum blade shape as a guide, select a blade shape that promises to be a good approximation. For ease of fabrication, linear variations of chord, thickness and twist might be chosen.

Calculate rotor performance and modify blade design

7. As outlined above the calculation of the rotor performance follows an iterative procedure to find the axial and angular induction factors. Initial guesses are needed and the values from an adjacent blade section or values from the previous blade iteration may be used. From the starting optimum blade design:

$$\varphi_{i,1} = tan^{-1}\left(\frac{2}{3\lambda_{r,i}}\right) \quad (23)$$

$$a_i, 1 = \frac{1}{\left[1+\frac{4sin^2(\varphi i,1)}{\sigma_{i,design}C_{l,design}\cos\varphi_{i,1}}\right]} \quad (24)$$

where σ is the local solidity or the ratio of the element area by the swept area defined as $\sigma = Bc/2\pi r_i$. The angular induction factor for the i*th* iteration is:

$$a'_{i,1} = \frac{1-3a_{i,1}}{(4a_{i,1})-1} \quad (25)$$

Having guesses for $a_{i,1}$ and $a'_{i,1}$, start the iterative solution procedure for the j*th* iteration. For the first iteration $j = 1$. Calculate the angle of the relative wind:

$$\tan\varphi_{i,j} = \frac{U\left(1-a_{i,j}\right)}{\Omega r\left(1+a'_{i,j}\right)} = \frac{1-a_{i,j}}{\left(1+a'_{i,j}\right)\lambda_{r,i}} \quad (26)$$

Determine $C_{l,i,j}$ and $C_{d,i,j}$ from the airfoil lift and drag data using:

$$\alpha_{i,j} = \varphi i, j - \theta_{p,i} \quad (27)$$

Calculate the local thrust coefficient

$$C_{T_r,i,j} = \frac{\sigma_i\left(1-a_{i,j}\right)^2\left(C_{l,i,j}\cos\varphi_{i,j}+C_{d,i,j}\sin\varphi_{i,j}\right)}{sin^2\varphi_{i,j}} \quad (28)$$

Update a and a' for the next iteration. If $C_{T_r,i,j} < 0.96$:

$$a_{i,j+1} = \frac{1}{\left[1+\frac{4sin^2\varphi_{i,j}}{\sigma_i C_{l,i,j}cos\varphi_{i,j}}\right]} \quad (29)$$

If $C_{T_r,i,j} > 0.96$:

$$a_{i,j} = 0.143+\sqrt{0.0203-0.6427\left(0.889-C_{T_r,i,j}\right)} \quad (30)$$

$$a'_{i,j+1} = \left[\frac{4cos\varphi_{i,j}}{\sigma C_{l,i,j}}-1\right]^{-1} \quad (31)$$

If the newest induction factors are within an acceptable tolerance of the previous guesses, then the other performance parameters can be calculated. If not, then the procedure starts again at Equation 26.

8. Having solved the equations for the performance at each blade element, the power coefficient is determined using:

$$C_P = \frac{8}{\lambda N}\sum_{i=k}^{N} sin^2\varphi_i\left(cos\varphi_i-\lambda_{r,i}sin\varphi_i\right)\left(sin\varphi_i+\lambda_{r,i}cos\varphi_i\right)\left[1-\left(\frac{C_d}{C_l}\right)cot\varphi_i\right]\lambda_{r,i}^2 \quad (32)$$

The total wind turbine thrust and torque is obtained by summing the results of the blade elements along the radial direction:

$$T = \sum_{i=k}^{N}\Delta T \quad (33)$$

$$Q = \sum_{i=k}^{N}\Delta Q \quad (34)$$

9. Modify the design if necessary and repeat steps 7-9 in order to find the best design for the rotor, given the limitations of fabrication.

3. PANEL METHOD

An efficient way of determining the C_l and C_d values required in the iterative solution of the previous section is through the panel method. Many authors such as Anderson (1991) and Chow (1979) have implemented the potential flow method for calculating pressure distributions around airfoil. The method presented by Anderson is based on the discretization of the airfoil surface in panels over which singularities such as vortexes and sources are placed. The flow pressures and velocities are calculated at the center of each panel (collocation point), where the contributions of the free stream flow and of each panel around the airfoil are summed up. The vortex and source strengths are then calculated using a linear system of equations in order to satisfy the boundary conditions. For the case studied here, the normal component of the velocity on each panel is considered to be 0. For the lifting flow case, another boundary condition is considered at the trailing edge where the tangential velocity at the panels on the upper and lower skins are made equal (one of the Kutta condition requirements).

According to the method presented by Anderson (1991) the Kutta condition applied at the trailing edge of the airfoil transforms the linear system of equations overdetermined. In order to solve this linear system, one of the equations representing the flow boundary condition applied to the control point of one of the panels must be ignored. The choice of what equation to ignore is difficult since it may introduce some arbitrariness in the numerical solution.

This problem is overcome in the methodology used by Houghton and Carpenter (2003) which mainly follows the original approach given by Hess and Smith (1967). Here, all the panels carry a source of strength σ_i and a vortex of strength γ. Since all the panels carry a vortex of equal strength the linear system of equations is easily solved adding one more term to the skin boundary condition and one more equation to satisfy the Kutta condition at the trailing edge making the system determined. Furthermore, the method used by Houghton and Carpenter (2003) for calculating angles between each panel and the flow is more practical than that presented by Anderson (1991) and Chow (1979) since it uses the vectorial dot product between the panel and the flow. This approach makes the calculations less prone to error once the sign of the trigonometric operators does not need to be taken into account in the numerical routines.

Figure 4 shows the comparison of the C_l vs. α curve for the NACA 23012 airfoil, which is commonly used for low Reynolds numbers applications. The experimental curve is given by Abbot and Doenhoff (1959). As it is shown, there is some correspondence of experimental and numerical values up to $\alpha = 10^o$, but the curves are detached from each other from $\alpha = 0^o$ up to the maximum α. This is due to the lack of viscous effects on the numerical model. Figure 4 also shows the pressure distribution on the upper and lower skins for $\alpha = 8^o$

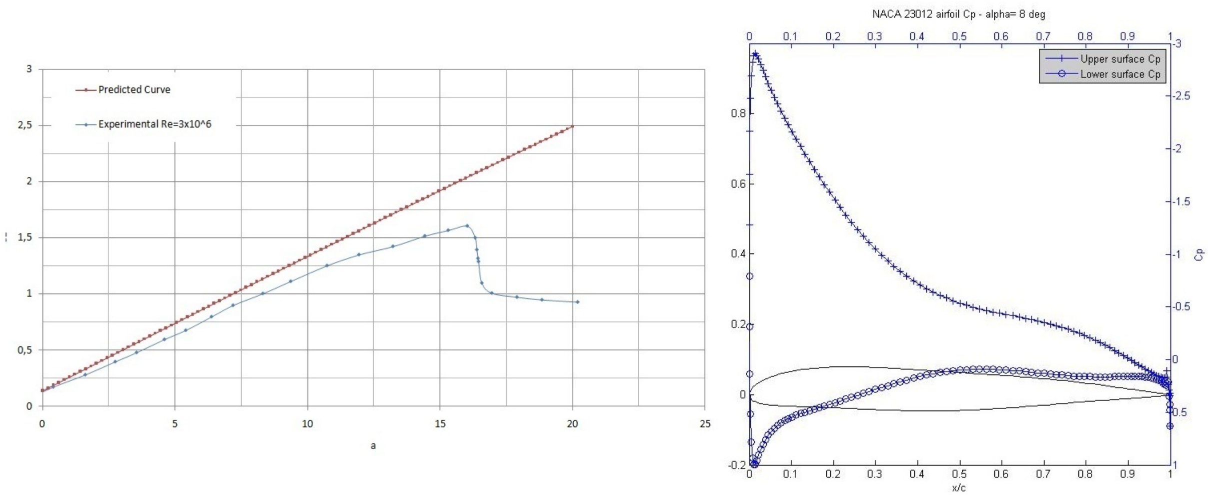

Figure 4. Comparison of C_l vs.α curves for NACA 23012 airfoil and airfoil pressure distribution.

In order to include viscous effects, some extra calculations must be made regarding laminar and turbulent boundary layers and transition points. For laminar boundary layers, Thwaitet's method is applied. In Thwaitet's method a simple single-order differential equation is integrated in order to provide the laminar boundary layer shape profile as a function of the dimensionless pressure gradient parameter. For turbulent boundary layers, Headt's method is applied. This method is rather empirical and is based in the study and fit of the profile of many turbulent boundary layers. In both methods the skin friction coefficient c_f is calculated.

According to Moran (1984), in the case of flow past an airfoil, the boundary layer starts out as laminar at the stagnation point, with a finite thickness. Sooner or later, all boundary layers become unstable, and any small disturbance initiates transition to the unsteady condition of turbulence. Transition starts at a particular value of the Reynolds number based on the distance x from the start of the boundary layer, the Re_x. For a boundary layer on a smooth plate, the critical value of Re_x is about 2.8×10^6. In fact the value of the transition Reynolds number depends on many factors such as the pressure gradient imposed on the boundary layer by the inviscid flow and surface roughness. Transition is hastened (Re_x is lowered) by both surface roughness and a positive value of dp/dx. For incompressible flows without heat transfer, Moran (1984) applies Michelt's method. According to this method, for airfoil-type applications, transition should be expected when:

$$Re_\theta > 1.174\left(1 + \frac{22400}{Re_x}\right) Re_x^{0.46} \tag{35}$$

where Re_θ is the Reynolds number calculated with a characteristic length called momentum thickness which relates the velocity inside the boundary layer with the free stream velocity. Finally the total drag coefficient is calculated with the skin friction drag and the form drag obtained from the pressure distribution of the inviscid calculations.

4. AIRFOIL PARAMETERIZATION

In order to perform the optimization of the airfoil shape to be used in a HAWT, such that the C_d/C_l ratio is minimized, a wide range of airfoil shapes, both known and unknown, must be analyzed. This can be done by means of a meta-model in which the C_d/C_l values of many airfoils are stored in a database and the optimization routine carries out the investigation of shapes present in the database in order to search the best airfoil for the proposed task. This methodology is presented by Menezes and Donadon (2009) and, usually, shapes are defined according to NACA series 4 and 5 geometries Ladson *et al.* (1996). Another approach is to parameterize the airfoil geometry according to desirable aerodynamic features. According to Mori *et al.* (2006) the changes implemented in the airfoil during a optimization procedure must be specified through geometric parameters instead of coordinates. These parameters can be used to define changes to the camber or the upper and lower skins of an airfoil profile.

In this paper, the methodology known as PARSEC by Sobieczky (1998) is implemented in order to apply changes to desirable features of the airfoil profile. Here, the airfoil is divided into a symmetric part and a camber line which are presented in the following polynomials:

$$t = a_1\sqrt{x} + a_2x + a_3x^2 + a_4x^3 + a_5x^4 \tag{36}$$

$$y_c = b_1x + b_2x^2 + b_3x^3 + b_4x^5 + b_5x^6 \tag{37}$$

In the above equations, all the coefficients are expressed in terms of 11 basic parameters: leading edge radius, upper crest location, lower crest location and curvature, trailing edge coordinate at $X = 1$, thickness, direction and wedge angle. Figure 5 shows the scheme for the eleven parameters and a comparison between the NACA 23012 actual and PARSEC representations with an estimated error of 0.59%.

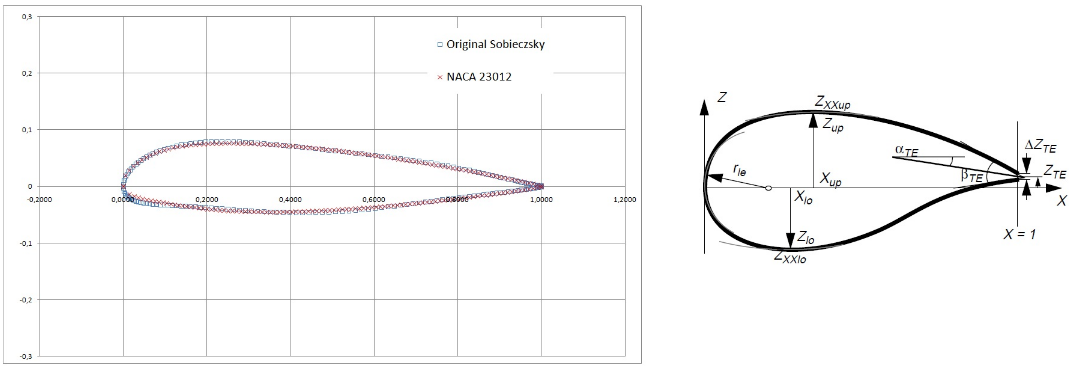

Figure 5. NACA23012 representation and PARSEC parameters

5. GENETIC ALGORITHM OPTIMIZATION

To optimize the cross-section used in the analysis of section 2with the specific section wind profile, a genetic algorithm optimization will be performed. The genetic algorithm is an heuristic method based on the biological concepts of natural selection and genetics. According to de Weck and Willcox (2004), in such scheme, for each interaction, the amount of changes termed as cross-overs, mutations and inheritance are set by the user and the choice of values to determine the PARSEC parameters is done randomly. After the current population is determined each individual is assessed in terms of the aerodynamic analysis of section 3. After that the more apt individuals are passed to the next generation of individual along with the most relevant features (genes).

6. CONCLUSIONS

This paper presented the guideline and preliminary results of a research aimed at optimizing a horizontal axis wind turbine from the aerodynamic standpoint. This optimization intends to enhance the power coefficient of a wind turbine blade including a phenomenon known as wake rotation. Effects like wing tip losses are not taken into account. The scheme to assess the blade power coefficient is termed blade element theory. In this theory, basic airfoil characteristics such as lift and drag coefficients are needed. For that, a panel analysis taking into account viscous effects is carried out for the varying conditions of each element. The airfoil section chosen for each blade element is then chosen by a genetic algorithm optimization aimed at minimizing the C_d/C_l ratio of the airfoil. Steps aimed at determining the drag coefficient of a generic airfoil with low Reynolds numbers are currently being implemented and the genetic algorithm optimization to obtain the best possible blade profile will be implemented further.

7. REFERENCES

Abbot, I.H. and Doenhoff, A.E.V., 1959. *Theory of Wing Sections*. Dover Publications, Inc., New York, NY, USA.

Anderson, J.D., 1991. *Fundamentals of Aerodynamics*. McGraw-Hill, Inc., New York, USA.

Chow, C.Y., 1979. *An Introduction to Computational Fluid Dynamics*. John Wiley & Sons, Inc., New York, NY, USA.

de Weck, O. and Willcox, 2004. "Lecture notes from the MIT multidisciplinary system design optimization open course". MIT open course web site <http://ocw.mit.edu/OcwWeb/Aeronautics-and-Astronautics/16-888Spring-2004/LectureNotes/index.htm>.

Hess, J.L. and Smith, A.M.O., 1967. "Calculation of potential flow about arbitrary bodies". *Progress in Aerospace Sciences*, Vol. 8, pp. 1–138.

Houghton, E.L. and Carpenter, P.W., 2003. *Aerodynamics for Engineering Students*. Butterworth-Heinemann, Oxford, UK.

Ladson, C.L., Brooks, C.W., Hill, A.S. and Sproles, D.W., 1996. "Computer program to obtain ordinates for naca airfoils". NASA Technical Memorandum 4741.

Manwell, J.F., McGowan, J.G. and Rogers, A.L., 2002. *Wind Energy Explained - Theory, Design and Application*. John Wiley & Sons, LTD, West Sussex, England.

Menezes, J.C. and Donadon, M.V., 2009. "Optimum blade design of a 2 mw horizontal axis wind turbine". In *Proceedings of the 20th Brazilian Congress of Mechanical Engineering*. Rio de Janeiro, Brazil, Vol. 1.

Moran, J., 1984. *An Introduction to Theoretical and Computational Aerodynamics*. John Wiley & Sons, Inc., New York, NY, USA.

Mori, A.K., Fico, N.G.C.R. and Mattos, B.S., 2006. "Multi-point wing design of a transport aircraft using a genetic algorithm". In *44th AIAA Aerospace Sciences Meeting and Exhibit*. Reno, Nevada, USA, Vol. 1.

Sobieczky, H., 1998. "Parametric airfoils and wings". *Notes on Numerical Fluid Mechanics*, Vol. 68, pp. 71–88.

8. RESPONSIBILITY NOTE

The authors are solely responsible for the contents of this imprint